SUPPLEMENTAL DATA

Correcting Smad1/5/8, mTOR, and VEGFR2 treats pathology in hereditary hemorrhagic telangiectasia models
Ruiz et al.

SUPPLEMENTAL FIGURES

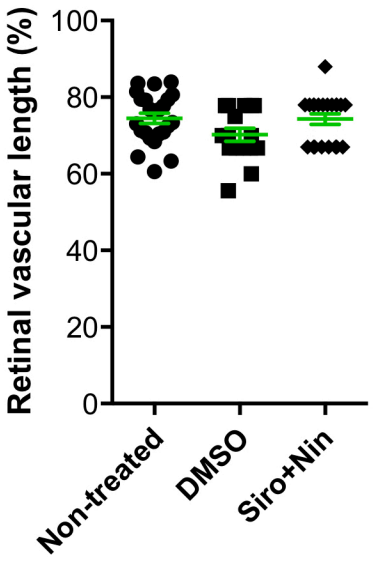

Figure S1. Siro+Nin does not affect normal vascular development in the mouse retina. Scatter plot shows retinal vascular length in P6 pups non-treated or treated with DMSO or Siro+Nin, as in Figure 1A. Data show the % of total retinal length occupied by the vasculature and represent mean ± SEM (n = 6, 4, 5 mice for the non-treated, DMSO, and Siro+Nin groups, respectively). One-way ANOVA and Tukey's multiple comparison tests revealed no significant difference between groups.

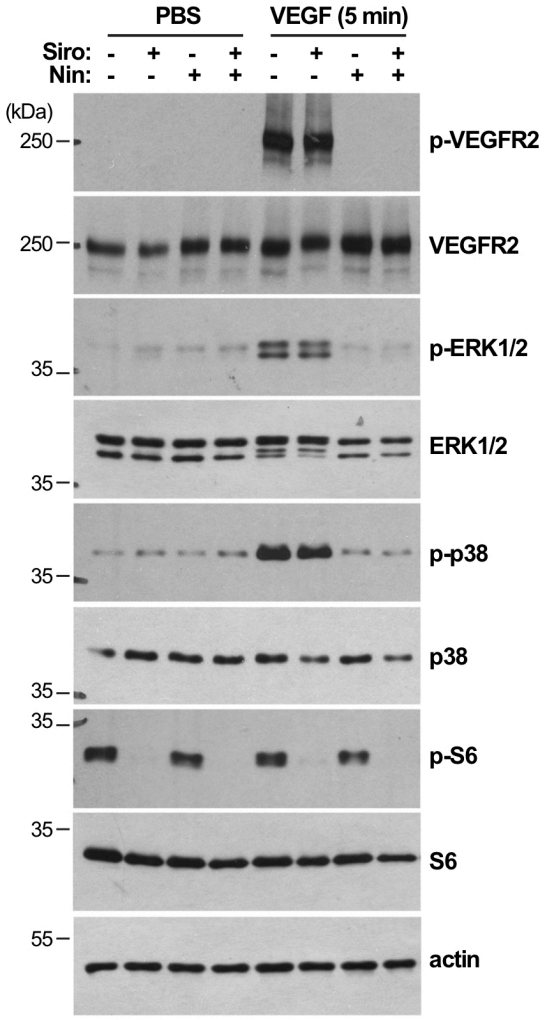

Figure S2. Siro does not inhibit VEGF-mediated ERK1/2 or p38 activation. HUVECs treated with vehicle [DMSO, (-)], Siro (300 nM), or Nin (300 nM), were stimulated for 5 min with VEGF (25 ng/mL), following a 24h starvation in 0.05% FBS-containing medium. Cell extracts were analyzed by WB using antibodies directed against the indicated proteins.

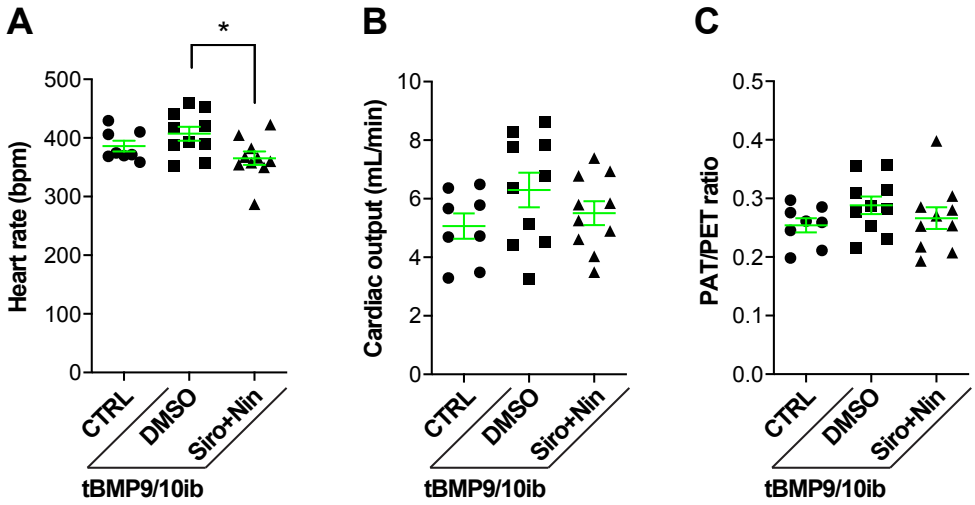

Figure S3. Siro+Nin does not affect cardiac function in tBMP9/10ib mice. Scatter plots show heart rate (A), cardiac output (B), and PAT/PET ratio (C) of P9 CTRL and tBMP9/10ib mice treated as in Figure 2A. Data represent mean ± SEM (n = 8, 10, 10 mice for the CTRL, DMSO, and Siro+Nin groups, respectively); one-way ANOVA, Tukey's multiple comparison test; **P*<0.05.

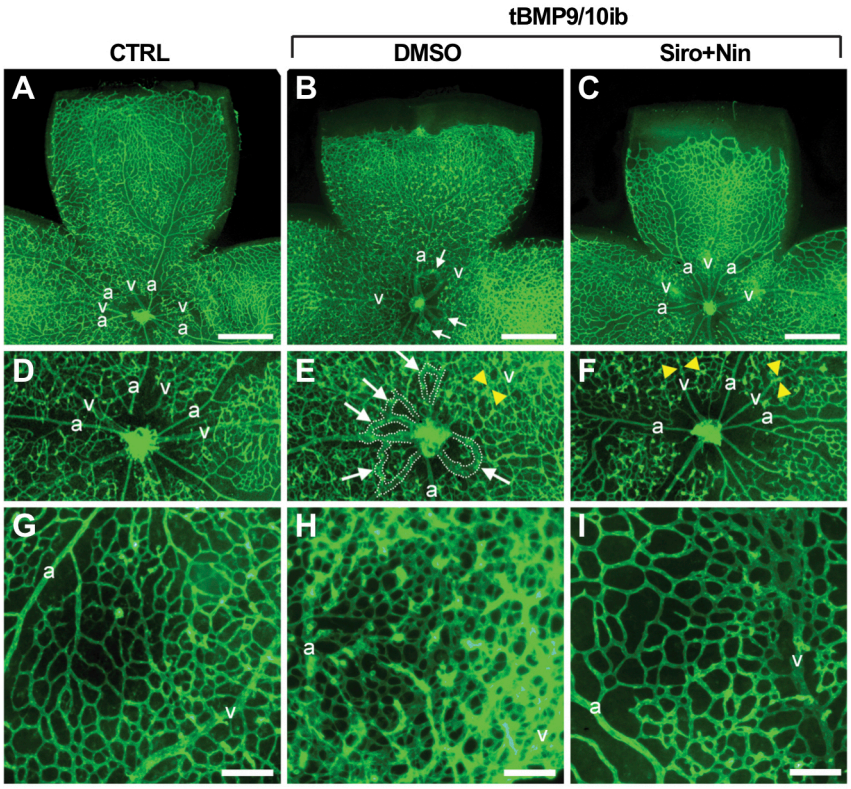

Figure S4. Siro+Nin prevents vein dilation, hypervascularization, and AVMs in the tBMP9/10ib mouse retina. (A-I) Representative images of retinas stained with fluorescent isolectin B4 (green) from P9 CTRL and tBMP9/10ib mice treated with DMSO and Siro+Nin, as in Figure 2A. Higher magnification in (D-F) shows retinal vein diameter [yellow arrowheads in (E and F) and retinal vascular fields (plexus area) between an artery (a) and a vein (v) (G-I). White arrows denote AVMs. Scale bars, 500 μm (A-C) and 100 μm (G-I).

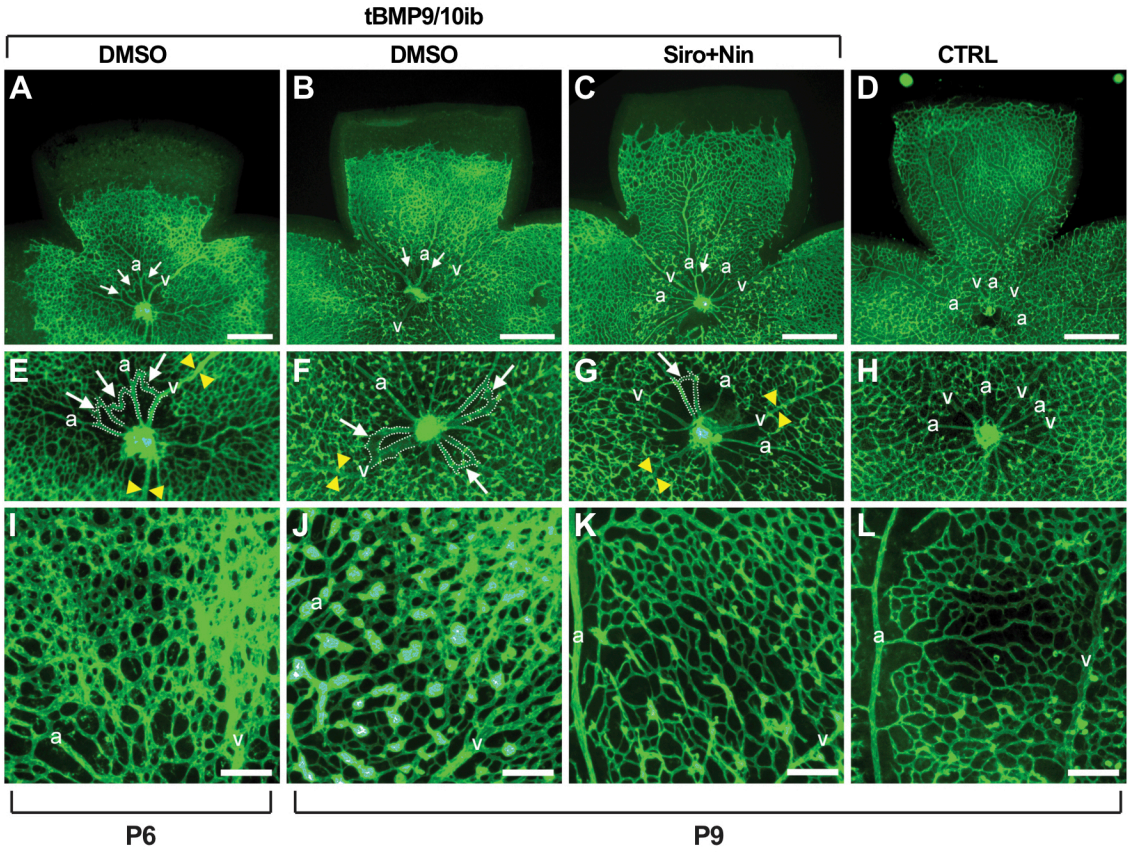

Figure S5. Siro+Nin reverses vein dilation, hypervascularization, and AVMs in the tBMP9/10ib mouse retina. (A-L) Representative images of retinas stained with fluorescent isolectin B4 (green) from CTRL and tBMP9/10ib mice (at the indicated postnatal day) treated with DMSO and Siro+Nin, as in Figure 4A. Higher magnification in (E-H) shows retinal vein diameter [yellow arrowheads in (E, F, and G)] and retinal vascular fields (plexus area) between an artery (a) and a vein (v) (I-L). White arrows denote AVMs. Scale bars, 500 μm (A-D) and 100 μm (I-L).

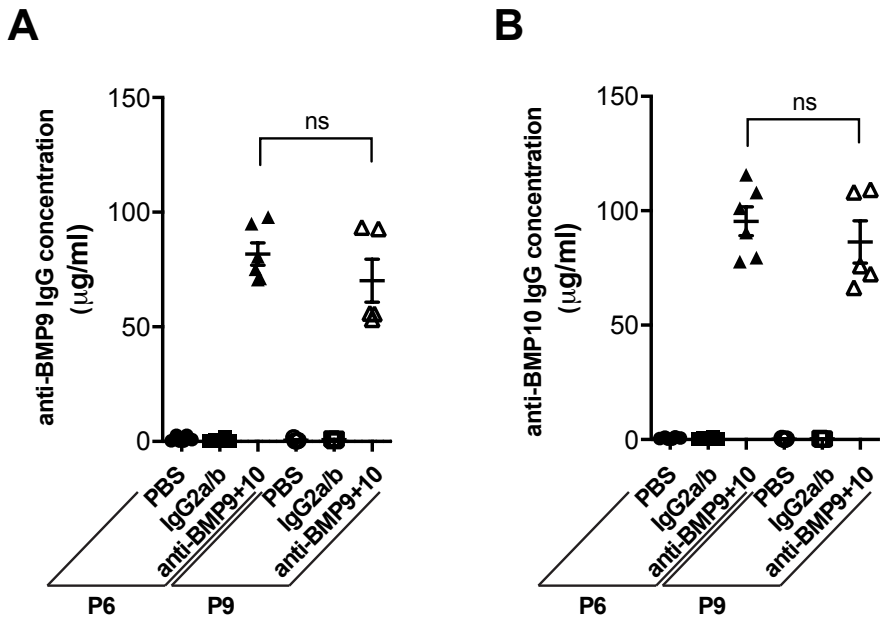

Figure S6. Transmammary-delivered BMP9 and BMP10 blocking antibodies persist in the circulation of mouse neonates. ELISAs were performed to measure anti-BMP9 **(A)** and anti-BMP10 **(B)** IgG concentration in the serum of P6 and P9 pups treated either at P3-P5 or P3-P8 through lactation from dams injected i.p. with PBS, isotype controls (IgG2a/b), or anti-BMP9 + anti-BMP10 antibodies (anti-BMP9+10). Data represent mean ± SEM (n = 6 and 5 mice for the P6 and P9 groups, respectively). One-way ANOVA and Tukey's multiple comparison tests revealed no significant difference between P6 and P9 mice for the anti-BMP9+10 groups.

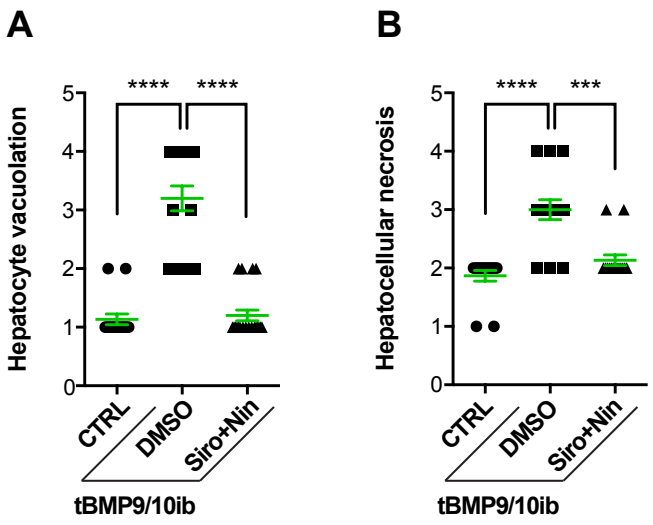

Figure S7. Siro+Nin attenuates hepatocyte toxicity in the liver of the tBMP9/10ib mice. Scatter plots of hepatocyte vacuolation **(A)** and hepatocellular necrosis **(B)** from liver of P9 control (CTRL) and tBMP9/10ib mice treated with DMSO and Siro+Nin, as in Figure 2A. Liver histological evaluation was performed according to the standardized semi-quantitative scoring system previously described (1). Data represent the mean of means ± SEM (5 random images of the liver per mouse, n = 3, 4, 4 mice for the CTRL, DMSO, and Siro+Nin groups, respectively); Kluskal-Wallis test, Dunn's multiple comparison test; ***P<0.001,****P<0.0001.

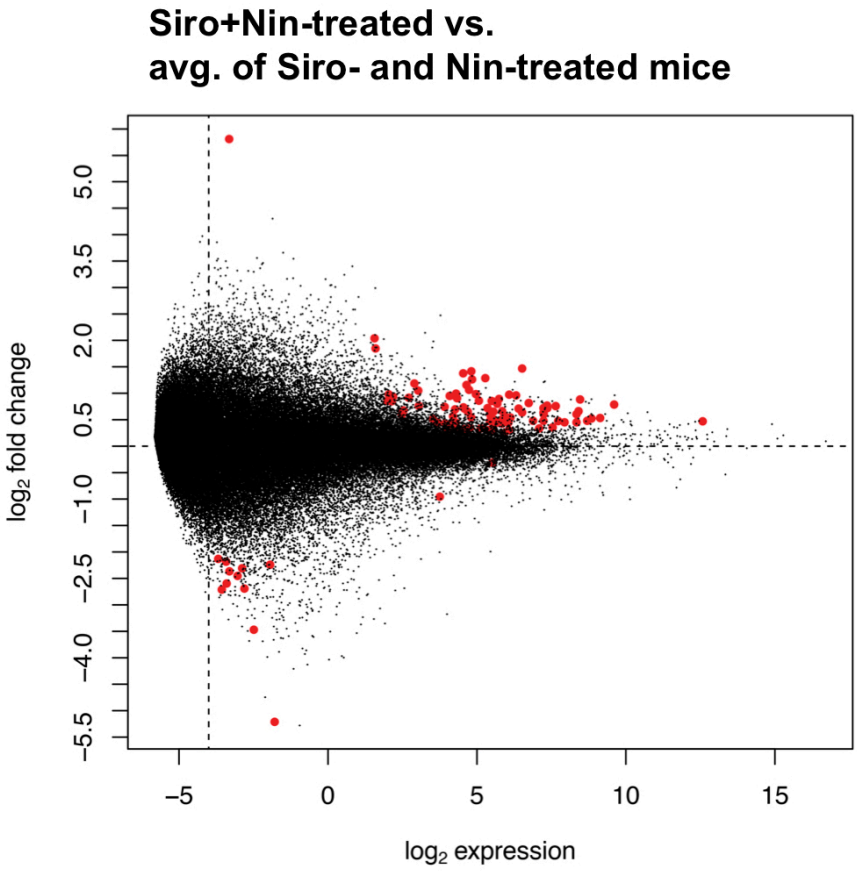

Figure S8. RNA-Seq quality control. We constructed an MA plot to visualize the effectiveness of the normalization and covariate control procedures employed during analysis of gene expression. The MA plot corresponds to the heatmap shown in Figure 7. The plot shows that the normalization and covariate adjustments employed were adequate for this dataset (most genes lie on a horizontal line corresponding to no change in gene expression with, as expected, more spread along the vertical for genes measured with low expression). Genes detected significant with a FDR≤1% are shown in red.

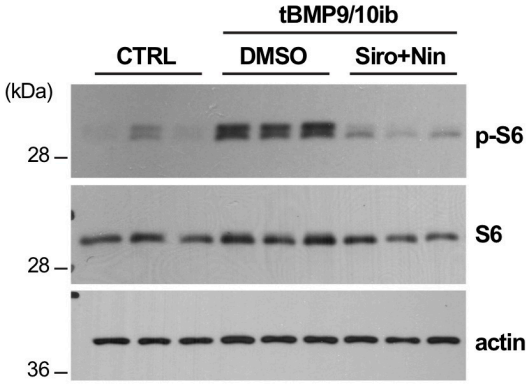

Figure S9. Siro+Nin inhibits S6 phosphorylation *in vivo* in tBMP9/10ib mice. P6 control (CTRL) and tBMP9/10ib mice were treated with DMSO or Siro+Nin, as in Figure 1A. Protein homogenates of whole liver were analyzed by WB using antibodies directed against the indicated proteins.

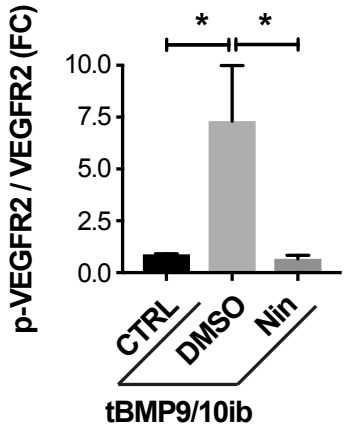

Figure S10. Nin prevents endothelial VEGFR2 overactivation *in vivo* in tBMP9/10ib mice. Densitometric analysis of the WB shown in Figure 9D quantifying phospho-VEGFR2 / total VEGFR2 ratio (p-VEGFR2/VEGFR2) in liver ECs isolated from CTRL and tBMP9/10ib mice treated with DMSO and Nin. FC, fold change. Data represent mean ± SEM (n = 5); one-way ANOVA, Tukey's multiple comparison test; **P*<0.05.

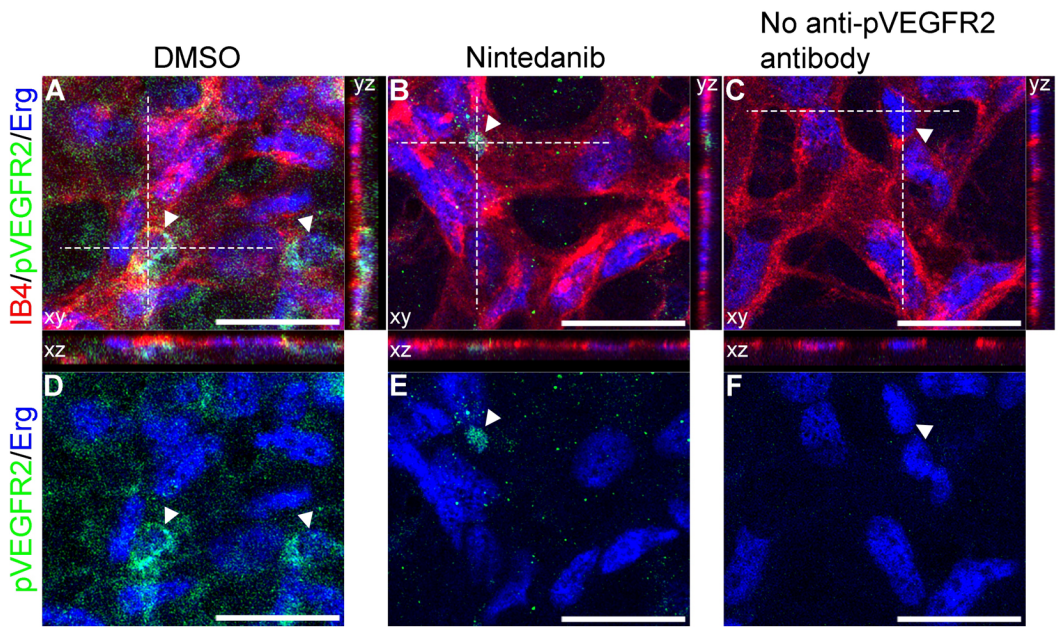

Figure S11. Nin prevents overactivation of endothelial VEGFR2 in tBMP9/10ib mice. The expression of p-VEGFR2 was analyzed by IHC in the retina of P6 tBMP9/10ib mice treated with vehicle (DMSO; A and D) and Nin (B and E). A control without primary antibody (no anti-pVEGFR2 antibody; C and F) was performed to evaluate the specificity of the anti-p-VEGFR2 antibody. Note the absence of fluorescent signal (green) from the secondary antibody used in the staining (C and F). Representative immunofluorescence images show the retinal vascular plexus stained with fluorescent isolectin B4 (red; A-C), anti-p-VEGFR2 (green; A-F), and anti-Erg (blue; A-F). Orthogonal views (xy, xz, and yz planes) show the superficial vascular plexus at the level of the dotted lines shown in (A, B, and C) and expression of p-VEGFR2 in endothelial cells (white arrowheads), see also focal plane views in (D, E, and F). Data represent an independent experiment with n = 2 and 3 mice for the DMSO and Nin groups, respectively. Scale bars, 25 μm.

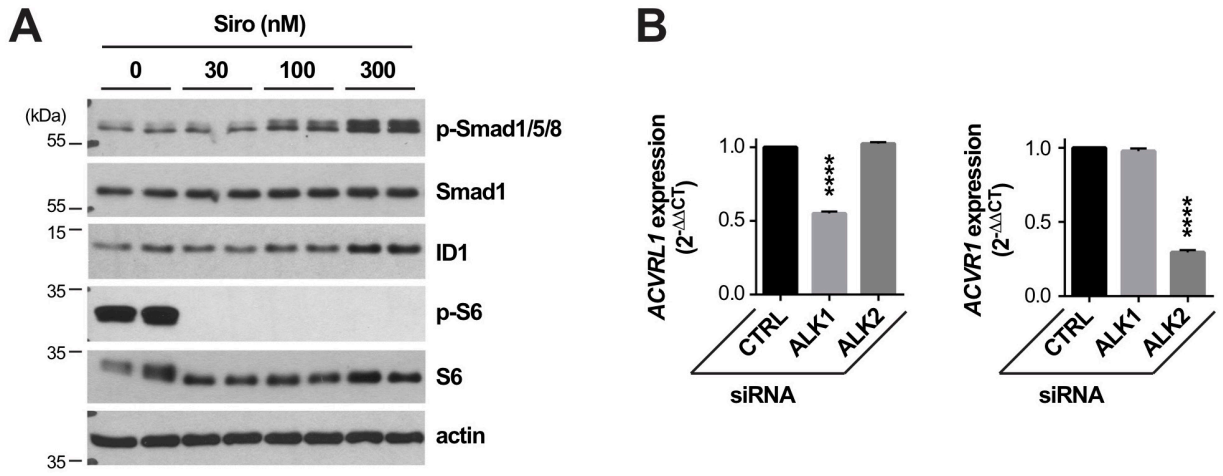

Figure S12. Siro rescues Smad1/5/8 signaling by activating ALK2. (A) C2C12 cells were treated for 3h with Siro in complete medium (conditioned for 2-3 days) and at the indicated concentrations. Cell extracts were analyzed by WB using antibodies directed against the indicated proteins. **(B)** Histogram showing *ACVRL1* (ALK1) and *ACVR1* (ALK2) expression ($2^{-\Delta\Delta Ct}$) in HUVECs treated with CTRL or *ACVRL1*- and *ACVR1*-targeting siRNA. Data represent mean ± SEM (n = 3); one-way ANOVA, Tukey's multiple comparison test; ****P<0.0001.

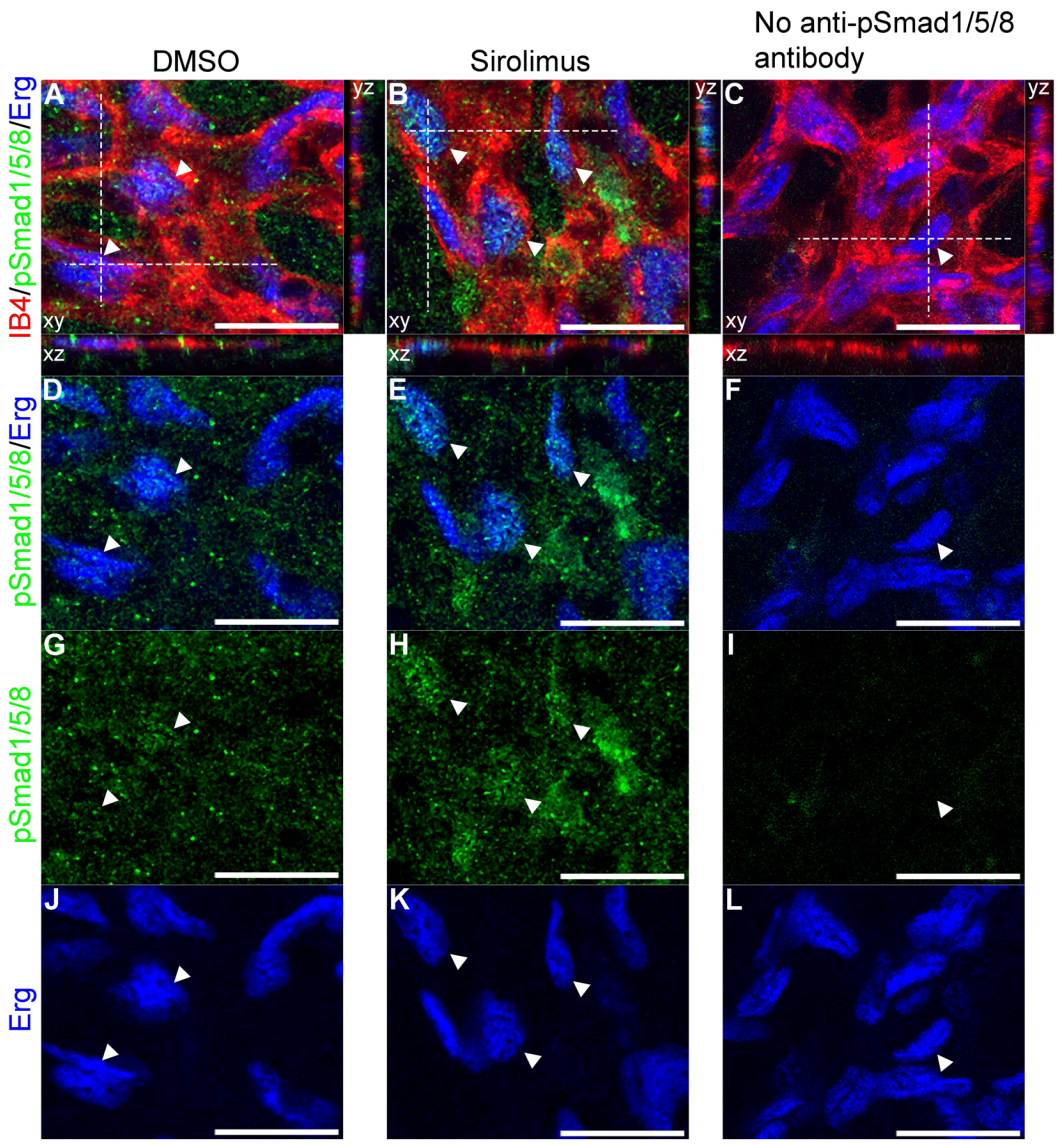

Figure S13. Siro rescues endothelial Smad1/5/8 signaling in tBMP9/10ib mice. p-Smad1/5/8 expression was analyzed by IHC in the retina of P6 tBMP9/10ib mice treated with vehicle (DMSO; A, D, G, and J) and Siro (B, E, H, and K). A control without primary antibody (no anti-pSmad1/5/8 antibody; C, F, I, and L) was performed to evaluate the anti-p-Smad1/5/8 antibody specificity. Note the absence of fluorescent signal for the secondary antibody used in the staining (C, F, and I). Representative immunofluorescence images show the retinal vascular plexus stained with isolectin B4 (red; A-C), anti-p-Smad1/5/8 (green; A-I), and anti-Erg (blue; A-F and J-L). Orthogonal views (xy, xz, and yz planes) show the superficial vascular plexus at the level of the dotted lines shown in (A, B, and C) and the expression of p-Smad1/5/8 localized mostly in the nuclei of endothelial cells (white arrowheads), see also focal plane views in (D-L). Data represent an independent experiment with n = 2 and 3 mice for the DMSO and Siro groups, respectively. Scale bars, 25 μm.

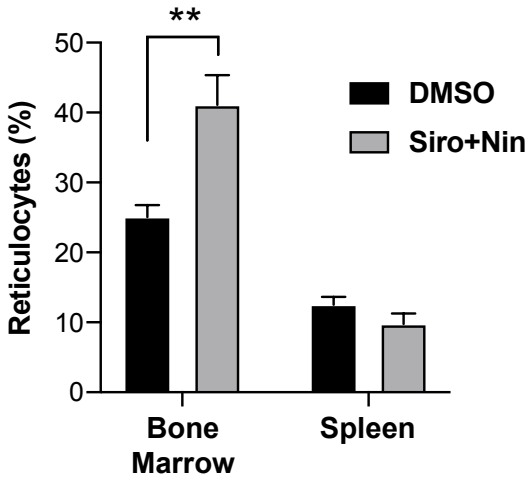

Figure S14. Siro+Nin increases the number of reticulocytes in the bone marrow of the tBMP9/10ib mice. Histogram shows reticulocyte counts determined in the bone marrow and spleen of P9 tBMP9/10ib mice treated as in Figure 2A with DMSO or Siro+Nin, and based on the expression levels of CD44 and Ter119, as described in (2). Data represent the mean of means ± SEM (n = 3 and 4 mice for the DMSO and Siro+Nin groups, respectively); two-way ANOVA, Bonferroni's multiple comparison test; $^{**}P<0.01$.

SUPPLEMENTAL TABLE LEGENDS

Table S1. Transcripts differentially expressed upon synergistic drug treatment. Transcripts shown in the heatmap of Figure 6 are presented in table form. Selection was the same as the heatmap: FDR≤0.5%, log average expression >-5. The transcripts were annotated with Biomart and ensembl genes 94 annotations.

SUPPLEMENTAL METHODS

Reagents and antibodies. BMP9 (3209-BP) and $VEGF_{165}$ (293-VE) were obtained R&D Systems. Sirolimus (Siro, S1039), nintedanib (Nin, S1010), and LDN-193189 (S2618) were from Selleck Chemicals. For WB, antibodies directed against p-S6 (4858), S6 (2217), p-Ser^{2448}-mTOR (2971), mTOR (2983), p-VEGFR2 (2478), VEGFR2 (2479), p-Smad1/5/8 (13820), Smad1 (9743), p-ERK1/2 (9101), ERK1/2 (9102), p-p38 (4511), and p38 (9212) were obtained from Cell Signaling Technology. Anti-ID1 antibody was from BioCheck (BCH-1/195-14). Anti-actin antibody was from BD Transduction Laboratories (612656). For IHC, anti-PAI-1 (ab66705), anti-HIF-1α (ab1), and anti-Erg (ab92513) antibodies were obtained from Abcam, anti-Ter119 antibody from R&D Systems (MAB1125), and anti-p-S6 (4858), anti-p-VEGFR2 (2478) and p-Smad1/5/8 (13820) antibodies from Cell Signaling Technology. Alexa Fluor 594 anti-rabbit or anti-rat goat secondary antibodies were used for IHC (Molecular Probes).

Transmammary-delivered immunoblocking of BMP9 and BMP10. For vascular disease induction in mouse pups, lactating dams were injected i.p. once at P3 with mouse monoclonal anti-BMP9 and anti-BMP10 antibodies (15 mg/kg bw, IgG2b, MAB3209; 15 mg/kg, IgG2a, MAB2926; R&D Systems, respectively), or with mouse monoclonal isotype controls (15 mg/kg, IgG2b, MAB004; 15 mg/kg, IgG2a, MAB003; R&D Systems) to obtain control mouse groups.

Measurements of antibody levels by ELISA in neonatal mouse serum. ELISAs were performed as described before (3), with the following modifications. 96-well ELISA plates (Maxisorp, Nunc) were coated with 100 µL of 1 µg/mL recombinant BMP9 or BMP10 (R&D Systems) in coating buffer (15 mM K2HPO4, 25 mM KH2PO4, 0.1 M NaCl2, 0.1 mM EDTA, 7.5 mM NaN3) and incubated overnight at 4 °C. Plates were then washed 3 times with 0.05% Tween PBS (PBST) and blocked for 1 h at room temperature (RT) with 1% BSA in PBS. After washing 3 times with PBST, serial dilutions of individual mouse serum samples and reference mouse anti-BMP9 and anti-BMP10 IgGs (R&D Systems) (diluted in 1% BSA PBS) were prepared and 100 µL/well were incubated for 2 h at RT. After 3 more washes, 100 µL/well horseradish peroxidase (HRP)-conjugated goat anti-mouse secondary antibody (Southern Biotech, diluted 1:500 in 1% BSA PBS) was incubated for 1 h at room temperature. TMB substrate was added after 5 washes and the reaction was allowed to develop for 30 min at room temperature. The optical density was measured at 450 nm using a TECAN GENios Pro plate reader.

Blue latex dye injection. P9 pups were processed for cardiac perfusion after euthanasia, following procedures described before (3). Briefly, the thorax and abdomen were opened. The left ventricles were injected manually with 600 µL of blue latex dye (BR80B, Connecticut Valley Biological Supply) using an insulin syringe U-100 (329652, BD Biosciences) and the right atrium was opened to drain the blood. After perfusion, liver, lungs, tongue, and palate were dissected, fixed in 4% paraformaldehyde (PFA), washed in phosphate-buffered saline (PBS) and either mounted in 80% glycerol (direct observation of the liver and lungs) or embedded in low gelling temperature agarose (A0701, Sigma) (tongue and palate). Blocks were dehydrated in methanol series and cleared with organic solvent (benzyl alcohol/benzyl benzoate, 1:1, Sigma). Images of the whole organ or tissue were acquired using an Olympus SZX7 stereomicroscope attached to an Olympus DP27 camera. Measurements and quantifications were performed using Fiji. For liver analysis, images from the

same liver lobe and at the same location in the lobe were acquired at 1x magnification. The diameter of every hepatic vessel was measured at a distance of 2,000 μm from the margin of the lobe using the concentric circle tool plugin in Fiji. For the tongue and palate, images of the organs were acquired using 2x magnification and transversal lines were superimposed half-way in their anterior-posterior axis using the grid Fiji's plugin, where the vessel diameter was measured. For the lungs, images of lobes were acquired and main vessels' diameter was measured. For some measurements, diameter of the same vessel was recorded at different levels of the palate, tongue, and lungs.

IHC. To analyze the retinal vasculature, eyes were enucleated and fixed in 4% PFA for 20 min on ice and retinas were isolated and analyzed as before (3, 4). Briefly, retinas were dissected, cut four times to flatten them into a petal flower shapes, and fixed with methanol for 20 min on ice. After removing methanol, retinas were washed in PBS for 5 min on a shaker at room temperature, and blocked in blocking solution (0.3% Triton, 0.2% BSA in PBS) for 1 h on a shaker at room temperature. Retinas were then incubated in Alexa Fluor 488 isolectin B4 (I21411, Molecular Probes) and/or primary antibodies in blocking solution on a shaker overnight at 4°C. Retinas were then washed four times in 0.3% Triton in PBS for 10 min on a shaker, incubated with the corresponding secondary antibodies, washed four times in 0.3% Triton in PBS for 10 min followed by two washes in PBS for 5 min on a shaker and mounted in Vectashield (H-1000, Vector Laboratories).

Liver, heart, and spleen were fixed in 4% PFA for 24 h and sent for sectioning, H&E staining, and anti-HIF-1α IHC at HistoWiz. Unstained liver sections were dewaxed and antigen retrieval was performed. Sections (5 μm) were then washed in PBS for 5 min on a shaker at room temperature, and blocked in blocking solution (0.3% Triton, 0.2% BSA in PBS) for 1 h in a humid chamber at room temperature. Immunostaining was performed using primary antibodies in blocking solution in a humid chamber overnight at 4°C. Sections were then washed four times in 0.3% Triton in PBS for 10 min, incubated with the corresponding secondary antibody, washed four times in 0.3% Triton in PBS for 10 min followed by one incubation with DAPI (KPL 710300) in PBS and two washes in PBS for 5 min on a shaker before being mounted in Vectashield.

High resolution images for vascular network analysis were acquired using a Zeiss 880 laser confocal microscope. In cases where low magnification was enough for the analyses, an automated EVOS FL Auto 2 Invitrogen microscope was used. Measurements, quantifications, and 3D analysis were performed using Fiji. Briefly, low magnification images were acquired using a 4x and 10x lens to measure the retina vascular length (percentage of vasculature/retina length). A 20x lens was used to acquire images at the optic nerve to quantify AVM number, and AVM and vein diameter, and at the vascular plexus (3-5 fields per retina, between an artery and a vein) to quantify the vascular density. All measurements and qualifications were done using Fiji. The vascular density quantification was done by using the measure particles tool, working with 8-bit images, adjusting the threshold, and measuring the area occupied by the vasculature in a region of interest of 200 x 200 μm^2. The bleeding area quantification was performed on 3 by 3 tiled image stacks using a 10x lens, and the 3D analysis by using the 3D project and the orthogonal view tools. Quantification of p-S6, p-VEGFR2, and p-Smad1/5/8 was performed by acquiring higher magnifications images using a 63x lens, analyzing 2 to 5 fields per retina and calculating the percentage of retinal vascular area occupied by immunostaining.

CBC. Blood samples from tBMP9/10ib mice were obtained through heart puncture using a 0.3 mL insulin syringe (324910, BD Biosciences). Blood was transferred to a tube containing 5 mM EDTA (Invitrogen) and HCT, RBC number, and Hb levels were determined on a Beckman Coulter AcT analyzer, no more than 30 min after blood collection.

Drug efficacy testing in adult Alk1 iKO mice. Tamoxifen was injected i.p. at 0.1 mg/g of body weight (b.w.) to 2-4 month-old $R26^{+/+}$;$Alk1^{2f/2f}$ (control group) and $R26^{CreER/+}$;$Alk1^{2f/2f}$ males and females on Day 0. Siro and Nin stock solutions were made in DMSO at 20 mg/mL and 10 mg/mL, respectively. The drugs were diluted in saline to 1X and adequate volume of drugs (Sir:Nin = 0.5:0.3 mg/kg bw) were injected i.p. once a day starting on Day 0. Saline containing 1% DMSO was used as vehicle control. Hb concentration in a drop of blood from tail snip was measured on Day 0, Day 7, and the last day (Day 9), using a Hb photometer (Hemopoint H2, STANBIO Laboratory). Any mice whose Hb levels were below 4 were subjected to termination on the day of measurement. At termination, mice were anesthetized by ketamine/xylazine (100/10 mg/kg bw), and GI tract was visually inspected and photographed. GI bleeding index was applied as 3 = severe; 2 = moderate; 1 = weak; 0 = none. Blood collected from abdominal vein was used for CBC on a HT5 Veterinary Hematology Analyzer (Heska). The whole body was fixed in formalin and bleeding was further inspected after collecting guts from stomach to rectum.

Cell cultures and RNAi. HUVECs were isolated from umbilical veins obtained from anonymous donors and subcultured in 5% fetal bovine serum (FBS)-containing EC growth medium (ScienCell), as described before (5). C2C12 cells were obtained from ATCC and were maintained in Dulbecco's Modified Eagle's Medium (DMEM) supplemented with 10% FBS, penicillin, and streptomycin. RNA interference (RNAi) was performed in HUVECs using Accell SMARTpool siRNAs targeting *ACVRL1* (E-005302-00) and *ACVR1* (E-004924-00), or using an Accell non-targeting pool control (D-001910-10), and by following the manufacturer's recommended protocols (Dharmacon).

Liver EC isolation. ECs were isolated from P9 mouse livers using anti-CD31 microbeads (Miltenyi Biotec GmbH), following the manufacturer's instructions.

WB analyses and proteomic array. For WBs, protein extracts were processed as before (4), with the following modifications. Cultured cells, isolated liver ECs, or whole liver tissue were solubilized in RIPA buffer (20-188, EMD Millipore) supplemented with 1× Complete protease inhibitor mixture (11697498001, Roche). 5-20 μg of proteins (depending on the primary antibody used) were separated by SDS-PAGE, transferred onto nitrocellulose membranes, which were probed with primary and secondary antibodies. A standard ECL detection procedure was used. For proteomic array, whole liver tissue homogenates were prepared and protein extracts were applied to the arrays following the manufacturer's instructions (ARY015, Proteome Profiler Mouse Angiogenesis Array Kit, R&D Systems).

RT-qPCR. Three days after siRNA treatment, cells were harvested and RT-qPCR was performed on pellets of ~100,000 cells per sample by using high capacity cDNA reverse transcription kit (Applied Biosystems) and by following the manufacturer's protocol. PCR was performed using TaqMan assays targeting *ACVRL1* (Hs00953798_m1), *ACVR1* (Hs00153836_m1) and *GAPDH* (Hs03929097_g1) on ABI 7900 HT (Applied Biosystems, Life Technologies). *ACVRL1* and

ACVR1 expression levels were normalized to the reference gene *GAPDH*. Relative changes in gene expression were determined by the ΔΔCt method and using control values normalized to 1.0.

RNA-Seq. Livers were rinsed with PBS and processed for RNA extraction using RNeasy mini kit (Qiagen), according to the manufacturer's instructions. Total RNA quality was verified using Thermo Scientific NanoDrop and Agilent Bioanalyzer. RNA was processed for RNA-Seq at the Genomics Resources Core Facility, Weill Cornell Medical College, New York, NY. Briefly, cDNA conversion and library preparation were performed using the TrueSeq v2 Illumina library preparation kit, following manufacturers' recommended protocols. Libraries were multiplexed 9 per lane and sequenced on 8 lanes of an Illumina HiSeq 4000 instrument. While the original and agreed upon design called for 8 lanes of sequencing in one run, the core facility sequenced these lanes in three separate runs, sequencing a subset of lanes twice, but not others. Analysis took this deviation into account by encoding which libraries had been sequenced with the altered design in the covariate matrix used for differential expression (the factor SEQUENCING_MOD encodes this information).

Gene expression differential expression analysis. RNA-Seq transcript counts were analyzed with analysis scripts written with the MetaR languages (6). Briefly, gene expression analysis used Limma Voom to estimate statistics of differential expression while correcting for covariates. Depending on the analysis, covariates included drug treatment, antibody used to induce the disease phenotype, and sequencing modality (e.g., libraries sequenced in a single lane by the core facility, or sequenced on two lanes in separate runs, then pooled). Disease phenotype consists of HEALTHY (or CTRL) and DISEASE (or tBMP9/10ib).

Model used for Figure 6 (statistical analysis and heatmap):
We fit the RNASeq read counts with Limma Voom using the following model:
Count ~ DRUG + ANTIBODY + SEQUENCING_MOD
Where Count is transcript read count; DRUG is COMBO=the Siro+Nin combination, SIRO=Siro alone, or NIN=Nin administered alone; ANTIBODY is tBMP9/10ib or CTRL, and SEQUENCING_MOD is sequencing modality. To identify genes whose expression indicate an interaction of the drug (synergistic effect), we selected genes for which the quantity (contrast for the statistical test of significance): COMBO - (SIRO+NIN)/ 2 significantly differed from zero. A contrast that differs from zero identifies genes whose expression changes are not additive with respect to the effect of each individual drug (because genes with additive drug effects would result in COMBO measuring the average expression across the drugs each administered alone). The MA plot for this differential expression analysis is shown in Figure S8.

Human BOECs isolation and characterization. BOECs were isolated as described before (4) from an HHT2 patient carrying the T372fsX truncation [*ACVRL1* c.1112dup, first reported in Ref. (7)].

Preparation of the standard and quality control solutions for liquid chromatography-mass spectrometry (LC-MS). Standard stock solution of Siro and Nin were prepared in DMSO and diluted with ion-free water to prepare working solutions at concentrations of 0.01, 0.1, 1, and 10 μg/mL. Standard solutions in a concentration range between 0 and 1000 ng/mL for Siro and between 0 and 2500 ng/mL for Nin were prepared diluting the working solutions with either 50%

MeOH in 5 mM ammonium formate water or 50% AcCN in 0.1% formic acid water, respectively. Quality control solutions used in the validation were prepared in the same manner as the standard solutions by using blank plasma collected from mice. All solutions were stored at -20°C before use.

Sample preparation and LC-MS analysis. Samples (calibrator, control, and plasma) were mixed either with a 70:30 mix of acetonitrile and 0.1 M zinc sulfate in water or with acetonitrile (for Siro and Nin samples, respectively), followed by vortex mixing for 30 sec. After mixing, samples were left at room temperature for 10 min and centrifuged (10,000 x g) for 10 min. The supernatant was dried under nitrogen and the residue was reconstituted either with 50 µL of 5 mM ammonium formate/MeOH (50:50%, v/v) or 40 µL of water/acetonitrile, with formic acid (0.1% v/v). Reconstituted residue was vortexed for 10 sec and centrifuged at 13,000 x g for 10 min. The final extract was transferred into polypropylene vials, and then 10 µL was injected and analyzed on a LTQ XL™ Linear Ion Trap MS coupled to a vanquish UHPLC system (Thermo Scientific), with a Accucore™ Vanquish™ C18+ UHPLC Column (1.5 µm, 2.1 x 50 mm) at 45ºC. A linear gradient of 50-100% methanol in 5 mM ammonium formate water (0.1% formic acid) or 2-95% acetonitrile was used for 6 and 10 min with flow rates of 0.2 and 0.4 mL/min, respectively. Data was analyzed using Xcalibur 3.1 (Thermo Scientific, USA), and Siro and Nin were identified through accurate mass measurements by comparison with pure standards. Peak areas of Siro and Nin were integrated and quantitated through the use of a calibration curve.

Cardiac ultrasound measurements and analysis. During ultrasound examination, mice were lightly anesthetized using isoflurane (3% induction dose, 1.5% maintenance dose) plus oxygen (1.5 L/min). Body temperature was maintained in a physiological range using build-in heat pad. Chest and upper abdominal hair was removed by a chemical hair remover (Nair, Church & Dwight Co., Inc, NJ); then, ultrasound gel was applied to the skin to facilitate sound transmission and to reduce contact artifacts. Echocardiography was done with a Vevo 3100 instrument (VisualSonics, Canada). MX550D high-resolution transducer was used under mouse (small) cardiology mode (frequency: 40 MHz; acquisition frame rate: 232 lps; gain: 29 dB; depth of penetration 10 mm; width: 12.08 mm) and color doppler mode (frequency: 32 MHz; PRF: 30 KHz; acquisition frame rate: 33 lps; gain: 30 dB). Measurement was performed using build-in cardiac package of RV and PV function to obtain parameters of heart rate (beats per min, BPM), cardiac output (mL/min) by LV area long under B-mode and LV area under M-mode, and PAT (ms), PET (ms), PAT/PET ratio under PW Doppler mode (8).

SUPPLEMENTAL REFERENCES

1. Fang H et al. Granulocyte colony stimulating factor induces lipopolysaccharide (LPS) sensitization via upregulation of LPS binding protein in rat. *PLoS One* 2013;8(2):e56654.

2. Chen K et al. Resolving the distinct stages in erythroid differentiation based on dynamic changes in membrane protein expression during erythropoiesis. *Proc. Natl. Acad. Sci. U. S. A.* 2009;106(41):17413–17418.

3. Ruiz S et al. A mouse model of hereditary hemorrhagic telangiectasia generated by transmammary-delivered immunoblocking of BMP9 and BMP10. *Sci. Rep.* 2016;5:37366.

4. Ruiz S et al. Tacrolimus rescues the signaling and gene expression signature of endothelial ALK1 loss-of-function and improves HHT vascular pathology. *Hum. Mol. Genet.* 2017;26(24):4786–4798.

5. Chatterjee PK, Al-Abed Y, Sherry B, Metz CN. Cholinergic agonists regulate JAK2/STAT3 signaling to suppress endothelial cell activation. *Am. J. Physiol. Cell Physiol.* 2009;297(5):C1294–306.

6. Campagne F, Digan WER, Simi M. MetaR: simple, high-level languages for data analysis with the R ecosystem. *bioRxiv* 2015;030254.

7. Abdalla SA, Cymerman U, Johnson RM, Deber CM, Letarte M. Disease-associated mutations in conserved residues of ALK-1 kinase domain. *Eur. J. Hum. Genet.* 2003;11(4):279–287.

8. Kohut A, Patel N, Singh H. Comprehensive Echocardiographic Assessment of the Right Ventricle in Murine Models. *J. Cardiovasc. Ultrasound* 2016;24(3):229–238.